ACS APPLIED MATERIALS & INTERFACES

Research Article

www.acsami.org

Interfacing Liquid Metals with Stretchable Metal Conductors

Bongsoo Kim,[†] Jaehyeok Jang,[†] Insang You,[‡] Jaeyoon Park,[†] SangBaie Shin,[‡] Gumhye Jeon,[§] Jin Kon Kim,*[,§] and Unyong Jeong*[,‡]

[†]Department of Materials Science and Engineering, Yonsei University, 50 Yonsei-Ro, Seodaemun-Gu, Seoul, Korea 120-749

[‡]Department of Materials Science and Engineering, Pohang University of Science and Technology (POSTECH), 77 Cheongam-Ro, Nam-Gu, Pohang, Gyeongbuk Korea 790-784

[§]National Creative Research Initiative Center for Smart Block Copolymers, Department of Chemical Engineering, Pohang University of Science and Technology (POSTECH), 77 Cheongam-Ro, Nam-Gu, Pohang, Gyeongbuk Korea 790-784

Supporting Information

ABSTRACT: Highly stretchable conductors are essential components in deformable electronics. Owing to their high stretchability and conductivity, liquid metals have attracted significant attention for use as circuits and interconnections. However, their poor wettability to stretchable metal electrodes prevents the formation of stable electrical connections. This study examined two approaches for creating a stable interface between a liquid metal (EGaIn) and stretchable metal electrodes via: (i) the use of honeycomb-structured stretchable metal electrodes and (ii) the addition of a conducting polymer interlayer. The line width of the honeycomb had a significant influence on the formation of a stable interface. The liquid metal formed a stable film layer on honeycomb metal electrodes, which have line widths of less than 50 μm. Coating PEDOT:PSS with a nonionic surfactant lowered the interfacial energy of EGaIn with flat stretchable metal surfaces; hence EGaIn was coated uniformly on the stretchable metal surfaces. Strain sensors were fabricated as a demonstrative example of an application that utilizes the stable interface.

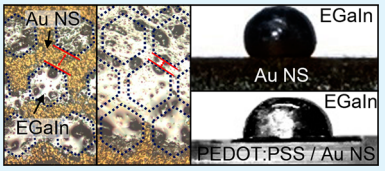

KEYWORDS: *liquid metal, EGaIn, stretchable conductor, wettability, interface, strain sensor*

INTRODUCTION

Wearable devices are expected to evolve to deformable electronics, which can maintain the stable performance of a device under high strains or during extreme body motions, such as folding, twisting, and stretching.[1] These deformable electronics will be applicable to a wide range of electronics including displays,[2−4] electronic skins sensing human motions, and external stimuli,[5−8] energy storage or generation devices,[9,10] and implantable devices for health monitoring.[11,12] The success of these new electronics depends on materials and their fabrication on elastomer substrates. As such, scientists have developed new materials or systems that can endure extreme mechanical deformations.[13,14]

Stretchable conductors are essential components in deformable electronics. Several approaches, such as conductive filler/elastomer composites,[15−18] metallic structures with in-plane or out-of-plane sinusoidal waves,[19−22] and direct wiring,[23] have been used to develop deformable conductors. Metals that are liquids (i.e., metallic liquids) at room temperature, including eutectic gallium−indium (EGaIn) and gallium−indium−tin (Galinstan), are considered promising materials for stretchable metallic circuits owing to their limitless stretchablilty and accompanying negligible change in electrical conductivity.[24−33] These liquids have low critical surface yield stresses (~0.5 N/m for EGaIn)[25] although a thin oxide layer (0.5−2.5 nm) forms rapidly when they are exposed to oxygen environments;[34−37] these low yield stresses allow the liquid metals to maintain their viscoelasticity in a wide range of mechanical strain. Two approaches have been formulated to fabricate stretchable circuits of liquid metals: (i) filling in an elastomer substrate through a syringe and (ii) printing on an elastomer surface. The former is problematic in miniaturized devices owing to the limited spatial resolution, whereas the latter allows the design of arbitrary circuits and offers improved spatial resolution. EGaIn has a reasonable adhesion to silicone-based elastomers, such as PDMS, and as such, patterning EGaIn on the PDMS substrate has been demonstrated in previous publications.[38,39] In addition, several printing techniques have been demonstrated with liquid metals including direct writing,[40] freeze-casting,[41] and three-dimensional printing of free-standing liquid metal microstructures.[42]

Liquid metals have excellent stretchability and conductivity, therefore they are well-suited for use as circuits and interconnections. However, creating interfaces between liquid metals and stretchable device electrodes has proven quite challenging. Figure 1A shows the contact angles of EGaIn on various substrates. These contact angles were measured at room temperature in a glovebox filled with nitrogen gas (oxygen concentration was less than 10 ppm). As previously reported,[34] the EGaIn droplet remained in the liquid state in this inert environment. Contact angles of 87°, 91°, 90°, 113°, and 119° were measured on a PDMS substrate, thermally evaporated flat

Received: December 17, 2014
Accepted: April 2, 2015
Published: April 2, 2015

DOI: 10.1021/am508899z
ACS Appl. Mater. Interfaces 2015, 7, 7920−7926

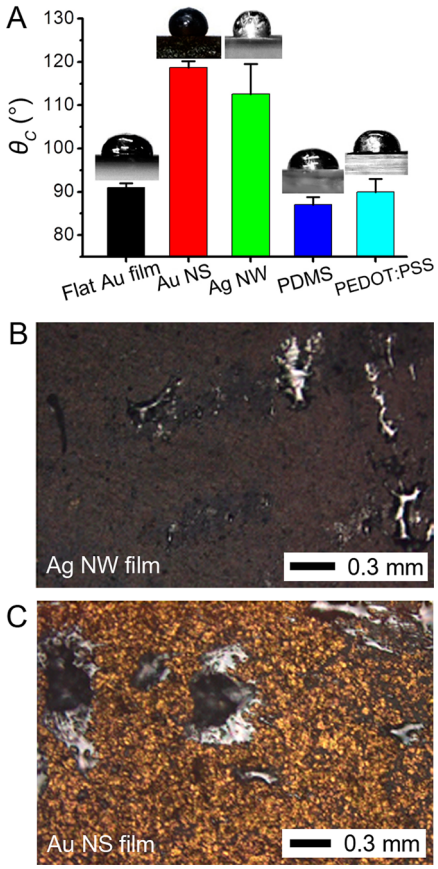

Figure 1. (A) Contact angles (θ_c) of EGaIn (eutectic GaIn) on various surfaces including a thermally evaporated flat Au film, stretchable Au nanosheet (NS) film, stretchable Ag nanowire (NW) film, a PDMS substrate, and a PEDOT:PSS film. (B, C) Dewetting of EGaIn on the films of Ag nanowire (B) and Au nanosheet (C).

Au film, flexible PEDOT:PSS conducting polymer film, stretchable Ag nanowire film, and stretchable Au nanosheet film, respectively. EGaIn was reasonably wetted on the flat Au film, the PEDOT:PSS film, and the PDMS surface but dewetted immediately after being coated on the Ag nanowire and Au nanosheet films (Figure 1B,C). This dewetting resulted mainly from hydrophilic surfactants, typically poly(vinylpyrollindone) (PVP) for the Ag nanowires[43] and the L-arginine for the Au nanosheets.[44] Increases in the contact angle are believed to result from the relatively large surface roughness of the nanowire and nanosheet films. In addition, when the contact angle was measured in ambient air, the droplets were somewhat solidified owing to the rapid oxidation of EGaIn (Supporting Information Figure S1). Dewetting of the gallium-based liquid metals prevents electrical connections with the electrodes.

Several techniques, such as the use of lyophobic surfaces,[39] embedding metal droplets in hydrophobic nanoparticles (i.e., liquid marbles),[45] and acid-impregnated surface,[46] have been proposed for improving the wettability of liquid metals. However, wetting of liquid metals on stretchable conductors has been scarcely studied, although the development of technologies that allow stable electrical connections between liquid metal circuits and stretchable metallic electrodes is essential for the fabrication of integrated stretchable devices. As such, this study proposes two methods for interfacing liquid metal and stretchable metal electrode patterns. These approaches include printing of the liquid metals on honeycomb-structured stretchable metal electrodes, and insertion of a conducting polymer interlayer between a flat stretchable metal electrode and the liquid metal. In addition, strain sensors are fabricated as a demonstrative example of an application that utilizes this stable interfacing.

RESULTS AND DISCUSSION

Solid−liquid adhesion can be quantified through contact angle hysteresis, which is the difference between the contact angles that a droplet makes while advancing (θ_A) on and receding (θ_R) from a surface.[47,48] The interfacial energies of EGaIn with the PDMS substrate were calculated as 0.51 N/m using the contact angle hysteresis ($\cos\theta_R - \cos\theta_A$), and with knowledge of the surface energies of the PDMS substrate (0.025 N/m).[49] This low interfacial energy resulted in easy patterning of the EGaIn on the PDMS surface, as shown in Figure 2A. Figure 2B shows

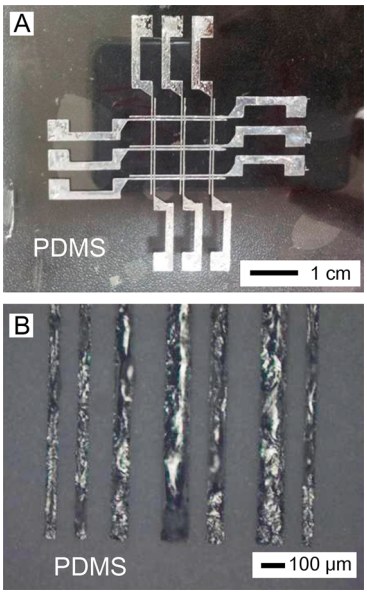

Figure 2. (A) Electrical circuit of EGaIn screen-printed on a PDMS substrate through a stencil mask. (B) Pattern of EGaIn with lines of different thicknesses and interspacing.

the line width achieved by screen printing, which was performed through a 50-μm-thick stencil mask. The line width of the liquid metal pattern was smaller than the opening of the mask, for example 35-μm-wide lines were obtained from a 50 μm-wide mask, owing to the poor wettability of the EGaIn with the stencil wall. In addition, for line widths less than 35 μm, the lines broke into small drops as a result of the liquid instability on the PDMS substrate.

When the stretchable metal conductors were coated on the PDMS surface, EGaIn dewetted on the metal surfaces. Wang et al. proposed a simple two-dimensional model for determining the dewetting condition of liquids coated on a surface consisting of nonwettable regions.[50] This model (shown in Figure 3) compares the total surface energy before and after dewetting by using the relation among the contact angle of the liquid on the nonwettable surface (θ_c), width of the nonwettable surface (L), thickness of the liquid (H), and the length of the periphery at the edge of the liquid (S). The liquid dewets on the nonwettable surface under the following condition:

DOI: 10.1021/am508899z
ACS Appl. Mater. Interfaces 2015, 7, 7920−7926

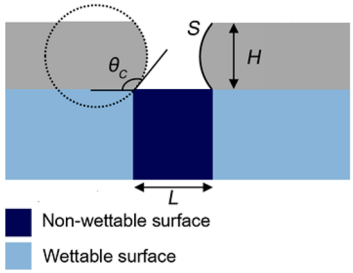

Figure 3. Two-dimensional model for calculating the critical dewetting condition. The periphery length (S) of EGaIn, was calculated by assuming that the periphery is semicircular.

$$L \geq S\frac{2}{1 - \cos\theta_c} \quad (1)$$

In this work, the thickness (H) of EGaIn (thickness of the stencil mask) is 50 μm. Critical L values were calculated to be 70 and 73 μm for contact angles of $\theta_c = 119°$ and $\theta_c = 113°$ on the flat Au nanosheet and Ag nanowire films, respectively. On the basis of the calculation, honeycomb patterns with a line width of 50 μm were prepared to prevent dewetting of EGaIn on the metal electrodes.

Figure 4 illustrates the procedure used to obtain the honeycomb metallic structure. The Au nanosheet honeycomb

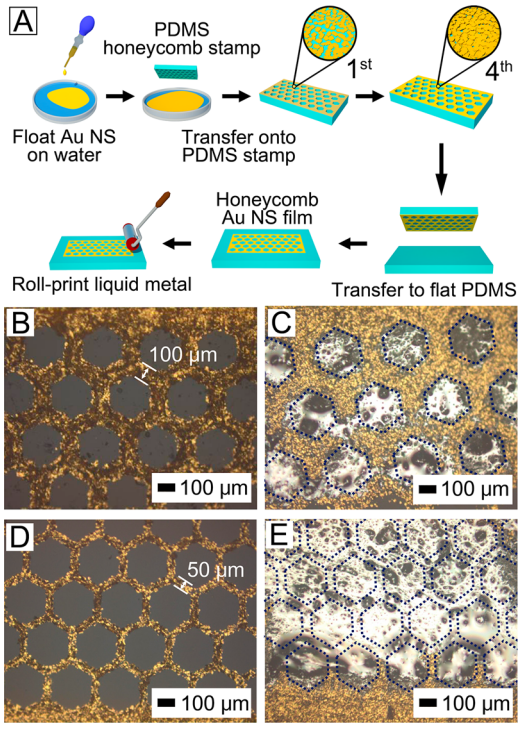

Figure 4. (A) Schematic of the procedure for obtaining a honeycomb pattern of Au nanosheets on a PDMS substrate. Au NSs were floated on water and transferred onto a PDMS stamp with a honeycomb design. The transfer was repeated four times on the same stamp. The Au NS honeycomb electrode on the stamp was transferred to a flat PDMS substrate. EGaIn was printed on the electrode by roll-printing. (B, D) Au nanosheet honeycomb patterns on PDMS substrates with line widths of 50 and 100 μm, respectively. (C, E) Optical images taken after roll-printing EGaIn. EGaIn was confined in the empty hexagons at 100 μm line width (C), but covered the entire honeycomb electrodes for line widths ≤50 μm (E).

structure was prepared as illustrated in Figure 4A, that is, we floated the Au nanosheets on water to prepare the Au nanosheet film, which was then transferred to a PDMS stamp. We transferred the Au nanosheets on to the PDMS stamp four times. Since the stretchability of the Au nanosheet film is attained by sliding between the nanosheets, reliable stretchability is obtained when 2−3 nanosheets are stacked. The overall thickness of the Au nanosheet was about 250 nm. Details of the stamping process and the corresponding stretchability are found in the previous report.[45] Since the continuous Au nanosheet film is stretchable up to ∼40% strain, the contribution of the honeycomb structure to stretchability is not critical in this study.

Figure 4B and D shows the honeycomb-shaped Au nanosheet electrodes. The honeycomb has 2D symmetry, which leads to an isotropic mechanical stress profile. This symmetry also results in maximum exposure of the PDMS surface and minimum surface occupation of the metals, which is critical to the adhesion of EGaIn to the PDMS surface and the prevention of dewetting. The wetting of EGaIn depends strongly on the design of the honeycomb (particularly the line width). For example, EGaIn islands (Figure 4C) were formed on the exposed PDMS surfaces when the line width of the honeycomb was 100 μm. A trace amount of EGaIn was pasted on a continuous Au nanosheet film by roll-printing, whereas the EGaIn covered the entire surface and made an excellent connection with the Au electrode when the line width was the same or less than 50 μm (Figure 4E). The threshold width, at which mechanical stability of the Au electrode is attained for strains of up to ε = 50%, was determined experimentally. A 30 μm-wide honeycomb pattern cracked at small strains (ε = 20%) near the front line with the liquid metal periphery, and hence was deemed too weak to be used as a stretchable electrode.

A similar procedure was applied to the Ag nanowire honeycomb pattern, as shown in Figure 5A. Ag nanowire was filtered on a filter paper (omnipore membrane filters, Merck Millipore Ltd.), and the film was transferred to a PDMS substrate. Poly(ε-carprolactone) (PCL), a low-melting point polymer (T_m = 60 °C), was spin-coated on a PDMS stamp with regular hexagonal features. The PCL-coated stamp was placed on the Ag nanowire film that had been preheated at 90 °C. After 1 min, the Ag nanowire film was cooled to room temperature. As a result, PCL molecules infiltrated the pores between the Ag nanowires and acted as a diffusive adhesive. The PDMS stamp was lifted off to leave the desired pattern behind on the PDMS substrate. The results of EGaIn wetting obtained here were very similar to those observed for the wetting on the Au nanosheet honeycomb-shaped electrodes, that is, EGaIn was confined (Figures 5B and C) to the PDMS surface for line widths of 100 μm or larger but covered the entire electrode surface for a line width of 50 μm (Figures 5D and E).

The second approach of interfacing EGaIn with metal electrodes includes the insertion of a PEDOT:PSS interlayer between the EGaIn layer and the metal electrodes. As shown in Figure 1A, the PEDOT:PSS has significantly lower contact angles than the stretchable metal conductors. We recently reported that adding small amounts of nonionic surfactant (Triton X-100) to an aqueous PEDOT:PSS solution enhances the coatability of PEDOT:PSS to both hydrophilic and hydrophobic surfaces.[51] This enhancement occurs since the hydrophobic part of the surfactant molecules binds to the metal surfaces, thereby resulting in a decrease in the interfacial energy

DOI: 10.1021/am508899z
ACS Appl. Mater. Interfaces 2015, 7, 7920−7926

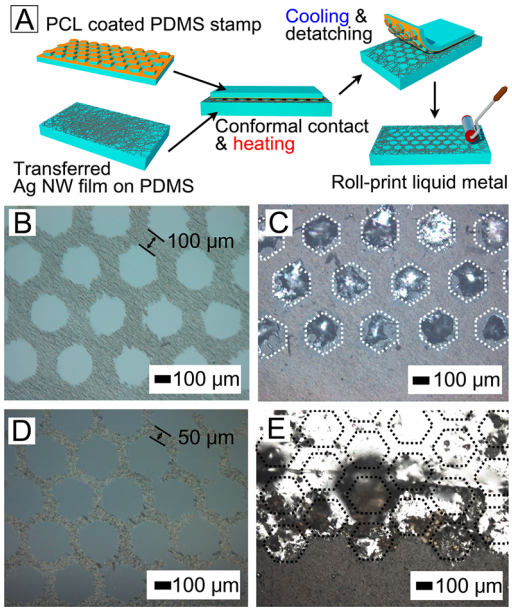

Figure 5. (A) Schematic of the procedure for obtaining a honeycomb pattern made of Ag nanowires (Au NWs) on a PDMS substrate. PCL was coated on a PDMS stamp with hexagonal pillars. The PCL-coated stamp was placed on a Ag NW film, and subsequently heated and cooled. Detaching the stamp left a Ag NW honeycomb electrode. (B, D) Ag NW honeycomb patterns with line widths of 100 and 50 μm, respectively. (C, E) Optical images taken after roll-printing EGaIn. EGaIn was confined in the empty hexagons at 100 μm line width (C), but covered the entire honeycomb electrodes for line widths ≤50 μm (E).

and an increase in the dispersive adhesion energy; this binding also occurs at the interface of PEDOT:PSS with EGaIn, regardless of the extent of oxidation of EGaIn at the interface. Figures 6A, B show the uniform coatings of EGaIn obtained via roll-printing on a PEDOT:PSS-coated Au nanosheet film (A) and Ag nanowire film (B). PEDOT:PSS was spray-printed through a mask on the stretchable metal electrodes. EGaIn was

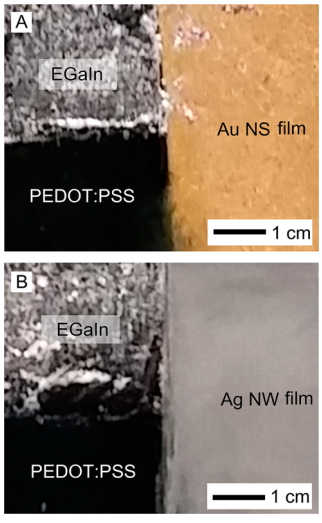

Figure 6. Optical images showing the EGaIn roll-printed on the films of PEDOT:PSS/Au NS (A) and PEDOT:PSS/Ag NW (B). EGaIn was printed on half of the PEDOT:PSS layers. EGaIn was not printed on the metal surfaces, but was uniformly coated on the PEDOT:PSS surface.

found only on the PEDOT:PSS layer, thereby forming a discrete boundary with the metal-only layers.

The contact resistance of the PEDOT:PSS interlayer was measured using the transmission line method (TLM).[52] The EGaIn electrode was printed on a thermally evaporated flat Au surface (50 nm in thickness) in order to measure the contact resistance between the EGaIn and the Au electrode. Figure 7

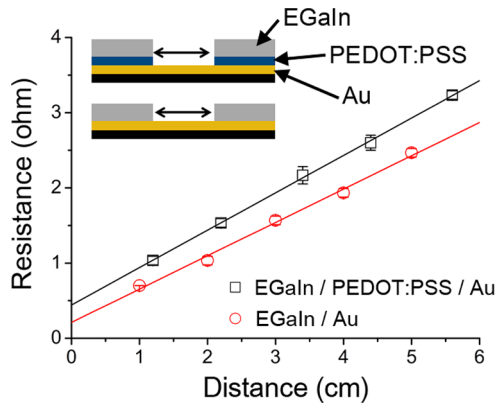

Figure 7. Areal contact resistance measurement via the transmission line method (TLM). The contact resistance between the EGaIn and the Au/PEDOT:PSS double layer was slightly higher than that between the Au film and the EGaIn.

shows the areal contact resistance measured at line distances of 1−6 cm between the EGaIn electrodes. The resistance between the Au film and EGaIn was measured as 0.055 Ω/mm^2. However, when EGaIn was printed on the Au/PEDOT:PSS double layer, the resistance increased slightly to 0.115 Ω/mm^2, which is sufficiently small for operating stretchable electronic devices.

We fabricated a stretchable LED array (Figure 8) to confirm the stability of the interface between the PEDOT:PSS

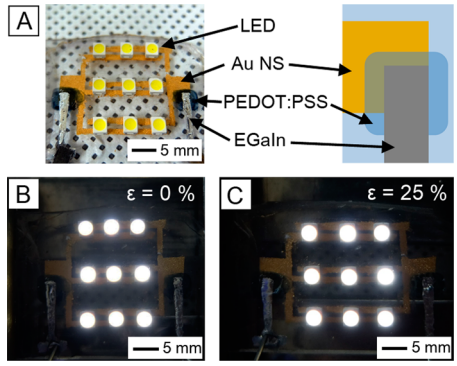

Figure 8. Demonstration of the stability of the interface between the EGaIn circuit and the Au/PEDOT:PSS double layer. (A) LED lamps were affixed to the comb-structured Au nanosheet electrode. (B, C) LEDs without strain (B) and at 25% strain (C).

interlayer and the EGaIn layer; that is, we fabricated a comb-structured Au nanosheet electrode pattern on a PDMS substrate and coated PEDOT:PSS exclusively on the electrode line. After thermal annealing at 140 °C for 10 min, the EGaIn circuit was screen-printed on the PDMS for partial coating on the Au/PEDOT:PSS electrode. LEDs were affixed to the comb electrode (Figure 8A). All of the components, including the interface between the EGaIn circuit and the electrode, were

DOI: 10.1021/am508899z
ACS Appl. Mater. Interfaces 2015, 7, 7920−7926

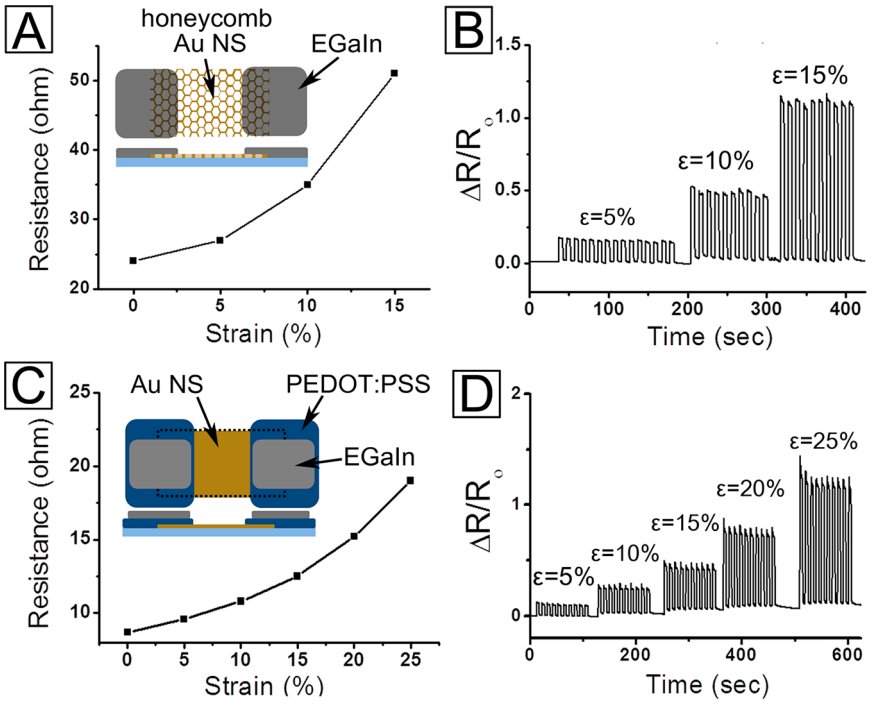

Figure 9. (A, B) Strain sensor constructed from the Au NS honeycomb and EGaIn as the sensing conductor and the stretchable circuit, respectively, and the corresponding sensing performance during repeated stretching cycles. (C, D) Strain sensor consisting of the Au NS solid film. PEDOT:PSS was coated on the Au NS pattern, and then EGaIn was roll-printed on the PEDOT:PSS surface. The strain sensor exhibited stable changes in the resistance.

stable for strains of up to 25% (Figure 8B and C). Furthermore, the intensity of the LED lights was constant during the stretching motions, which indicates that the interface between the EGaIn and the metal is mechanically stable.

Owing to their negligible change in conductivity during mechanical deformation, EGaIn circuits are ideal for use in strain sensors operating under high strains; therefore as a demonstrative exercise, these EGaIn circuits interfacing stretchable metal conductors were installed for use in strain sensors (Figure 9). Liquid metals themselves can be used as sensing materials. In fact, liquid-metal-based strain sensors are quite reliable since their currents change linearly with the applied strain. Although sensors that operate via percolation are not highly reliable at high strains, they are more sensitive to strain compared with their liquid-metal-based counterparts. For example, the liquid metal strain sensor exhibited $\Delta R/R_o$ of ~0.02 at 10% strain,[53] but the sensor in this study showed $\Delta R/R_o$ of 0.5 at the same strain. Therefore, sensing materials of strain sensors should be selected on the basis of the target sensing strain and the required sensitivity. In the case of the sensor, which is composed of the honeycomb sensing electrode connected to the EGaIn circuit, Figure 9A and B shows that the resistance increases linearly for strains of up to ε = 15% ($\varepsilon = \Delta L/L_o \times 100$ when L is the length of specimen along the elongational direction), and sharply thereafter; this honeycomb structure has a line width of 50 μm. This type of sensor was highly reliable for strains of up to ε = 20% and mechanically induced electrical failure did not occur in any of the ten samples (i.e., 10 sensors) we tested. Figure 9B shows the high stability of the sensor during the repeated strain cycles; the initial resistance was completely restored for a strain of ε = 20%. Moreover, the resistance of the sensor constructed from a PEDOT:PSS-coated Au nanosheet line, which was covered by EGaIn, increased linearly (Figure 9C and D) with strains of up to ε = 25%, and at faster rates thereafter. In general, this sensor exhibited a reliable response to strains of up to 30%. The strain-dependent resistance hysteresis during a cycle of strains was negligible in the honeycomb approach. When PEDOT:PSS interlayer was used, small hysteresis was obtained. (Supporting Information Figure S3)

CONCLUSION

The poor wettability of EGaIn to the stretchable metal electrodes was improved by introducing two methods of interfacing, hence stable interface was created between the EGaIn and the stretchable metal electrodes. We used Au nanosheet and Ag nanowire electrodes as the stretchable electrodes. The use of honeycomb structure on a PDMS substrate was effective when line widths of the honeycomb was the same or less than 50 μm, whereas EGaIn formed droplet islands (instead of a continuous film) when the line width was 100 μm. Coating PEDOT:PSS blended with a nonionic surfactant (Triton X-100) on the metal electrodes facilitated the wetting of EGaIn, which created a stable interface with the stretchable metals. The contact resistances between the metal and EGaIn were small enough in both approach for stretchable lighting. The strain sensors based on the stable interface between the EGaIn circuit and metal electrodes exhibited highly reliable sensor performance. This concept has the potential for application to other conductors.

EXPERIMENTAL SECTION

Materials. A liquid metal (eutectic gallium indium: EGaIn), PCL (polycaprolactone, M_w = 42500), octadecyltrichlorosilane (OTS, ≥90%), tetrahydrofuran (THF, 99.5%), *N*,*N*-dimethylformamide (DMF, ≥99%), and 1-butanol (≥99%), 2-mercaptopropanoic acid (MPA, ≥99%), hydrogen tetrachloroaurate trihydrate ($HAuCl_4 \cdot 3H_2O$, 99%), silver nitrate ($AgNO_3$, 99.5%), L-arginine, and Triton X-100

DOI: 10.1021/am508899z
ACS Appl. Mater. Interfaces 2015, 7, 7920−7926

were purchased from Sigma-Aldrich. In addition, poly(dimethylsiloxane) (PDMS) and a PEDOT:PSS solution (Clevious P) were purchased from Dow Corning and Heraeus, respectively.

Patterning the Honeycomb-Structured Au Nanosheet Film. Au nanosheets were synthesized at 95 °C in an aqueous solution containing hydrogen tetrachloroaurate trihydrate ($HAuCl_4 \cdot 3H_2O$) and L-arginine.[44] A monolayer film of the nanosheets was obtained by via the process described in our previous publication.[54] The Au nanosheets, dispersed in 1-butanol, were dropped on D.I. water until a macroscopic monolayer film formed. The honeycomb-shaped PDMS stamp was prepared by spin-coating SU-8 (MicroChem) on an O_2-plasma-treated silicon wafer and then etched by standard lithography to form 80 μm (height) × 120 μm (lateral side length) SU-8 hexagonal pillars. The pillars were spaced 50, 75, 100, and 150 μm (Supporting Information Figure S2) apart, depending on the prepared stamp. The PDMS prepolymer was poured on the SU-8 pattern, cured at 180 °C in vacuum, and filed off to prepare the stamps. Moreover; the Au nanosheet film, floating on the water surface, was transferred to the PDMS stamp through simple contact with the film. This transfer was repeated three times in order to attain reliable stretchability.[44] The Au nanosheet pattern on the stamp was subsequently transferred to a semicured PDMS substrate, which was then was fully cured at 180 °C. All of the PDMS elastomers were prepared by mixing the base monomer and a curing agent at weight ratios of 10:1 (w/w).

Patterning the Honeycomb-Structured Ag Nanowire Film. Ag nanowire was synthesized via a procedure described in the literature.[43] The Ag nanowires were dispersed in ethanol and the suspension was vacuum filtered to form a dense film on the filter paper (filter type = 0.2 μm JG). This nanowire film was then transferred to a flat PDMS substrate. A PCL solution (3 wt % in chloroform) was spin-coated on a PDMS stamp with a periodic array of 80 μm (height) × 120 μm (lateral side length) hexagonal pillars. These pillars were spaced 50 μm, 75 μm, 100 μm, and 150 μm, apart, depending on the stamp. The PCL-coated stamp was placed on the Ag nanowire film, heated to 90 °C for 1 min, and then cooled to 10 °C. The PDMS stamp was subsequently lifted off leaving behind the Ag nanowire honeycomb film on the flat PDMS substrate.

Printing EGaIn. A stencil Ni mask was placed on the stretchable metal conductor pattern, and EGaIn was roll-printed on the conductor with a small paint roller. Triton X-100 was dissolved in water (1.0 wt %) and a commercial PEDOT:PSS solution (Clevious P, Heraeus, solute concentration = 1.3 wt %) was mixed with this solution in an equal volume ratio. This blended solution was selectively deposited onto the electrodes or around the rubber-electrode interface and the resulting films were thermally annealed at 140 °C for 10 min in air. The EGaIn was screen printed with a 50-μm-thick stencil Ni mask.

Contact Angle Measurement. EGaIn is oxidized rapidly under ambient conditions.[34] We measured the contact angles in a glovebox that was filled with N_2 (99.998%) after vacuum evacuation. The oxygen concentration was maintained at <10 ppm during the measurement. EGaIn droplets were placed on the surfaces of a thermally evaporated flat Au thin film, Au nanosheet film, Ag nanowire film, PDMS substrate, and PEDOT:PSS-coated Au nanosheet film. The resulting contact angles were obtained from a digital image, which was taken inside the glovebox by using a digital camera (60D, Cannon).

Strain Sensor Measurement. Both ends of the stretchable metal pattern were interfaced with the EGaIn pattern. For straightforward measurements, a metal wire was placed on the end of the EgaIn pattern and the samples were then fully embedded in a 1 mm-thick PDMS plate. The resistance between the two EGaIn circuits was measured at strains ranging from 5%−25%.

Characterization. The surface tension was determined, optical images were obtained, and the electrical resistance was measured using an optical tensiometer (Biolin Scientific, Attension Theta Auto 3), an Olympus BX-51 microscope, and an I−V Source meter (Keithley 2400), respectively.

■ ASSOCIATED CONTENT

Ⓢ Supporting Information

EGaIn droplet images on various surfaces under ambient conditions, images of the honeycomb molds with different sizes and line widths, and cyclic test of the resistance versus strain. This material is available free of charge via the Internet at http://pubs.acs.org.

■ AUTHOR INFORMATION

Corresponding Authors

*Email: jkkim@postech.ac.kr.
*Email: ujeong@postech.ac.kr.

Author Contributions

B.K. and J.J. contributed equally to this work.

Notes

The authors declare no competing financial interest.

■ ACKNOWLEDGMENTS

This work was supported by the Ministry of Science, ICT and Future Planning (MSIP), Korea, under the "IT Consilience Creative Program" (NIPA-2013-H0203-13-1001) supervised by the NIPA.

■ REFERENCES

(1) Rogers, J. A.; Curvy, Y. A. Stretchy Future for Electronics. *Proc. Natl. Acad. Sci. U. S. A.* **2009**, *106*, 10875−10876.
(2) Sekitani, T.; Nakajima, H.; Maeda, H.; Fukushima, T.; Aida, T.; Hata, K.; Someya, T. Stretchable Active-Matrix Organic Light-Emitting Diode Display Using Printable Elastic Conductors. *Nat. Mater.* **2009**, *8*, 494−499.
(3) Liang, J. J.; Li, L.; Niu, X. F.; Yu, Z. B.; Pei, Q. B. Elastomeric Polymer Light-Emitting Devices and Displays. *Nat. Photonics* **2013**, *7*, 817−824.
(4) White, M.; Kaltenbrunner, M.; Glowacki, E.; Gutnichenko, K.; Kettlgruber, G.; Graz, I.; Aazou, S.; Ulbricht, C.; Egbe, D. A. M.; Miron, M. C.; Major, Z.; Scharber, M. C.; Sekitani, T.; Someya, T.; Bauer, S.; Sariciftci, N. S. Ultrathin, Highly Flexible and Stretchable PLEDs. *Nat. Photonics* **2013**, *7*, 811−816.
(5) Yamada, T.; Hayamizu, Y.; Yamamoto, Y.; Izadi-Najafabadi, A.; Futaba, D. N.; Hata, K. A Stretchable Carbon Nanotube Strain Sensor for Human-Motion Detection. *Nat. Nanotechnol.* **2011**, *6*, 296−301.
(6) Pang, C.; Lee, G.-Y.; Kim, T.; Kim, S. M.; Kim, H. N.; Ahn, S.-H.; Suh, K.-Y. A Flexible and Highly Sensitive Strain-Gauge Sensor Using Reversible Interlocking of Nanofibres. *Nat. Mater.* **2012**, *11*, 795−801.
(7) Chortos, A.; Bao, Z. Skin-Inspired Electronic Devices. *Mater. Today.* **2014**, *17*, 321−331.
(8) Lu, N.; Kim, D.-H. Flexible and Stretchable Electronics Paving the Way for Soft Robotics. *Soft Robotics* **2013**, *1*, 53−62.
(9) Hu, L.; Pasta, M.; La Mantia, F.; Cui, L.; Jeong, S.; Deshazer, H. D.; Choi, J. W.; Han, S. M.; Cui, Y. Stretchable, Porous, and Conductive Energy Textiles. *Nano Lett.* **2010**, *10*, 708−714.
(10) Cho, J.; Lee, J.; Huang, X.; Jia, L.; Fan, J. A.; Su, Y.; Su, J.; Zhang, H.; Cheng, H.; Lu, B.; Yu, C.; Chuang, C.; Kim, T.; Song, T.; Shigeta, K.; Kang, S.; Dagdeviren, C.; Petrov, I.; Braun, P. V.; Huang, Y.; Paik, U.; Rogers, J. A. Stretchable Batteries with Self-Similar Serpentine Interconnects and Integrated Wireless Recharging Systems. *Nat. Commun.* **2013**, *4*, 1543.
(11) Kim, D.-H.; Ghaffari, R.; Lu, N.; Rogers, A. J. Flexible and Stretchable Electronics for Biointegrated Devices. *Annu. Rev. Biomed. Eng.* **2012**, *14*, 113−128.
(12) Kim, J.; Lee, M.; Rhim, J. S.; Wang, P.; Lu, N.; Kim, D.-H. Next-Generation Flexible Neural and Cardiac Electrode Arrays. *Biomed. Eng. Lett.* **2014**, *4*, 95−108.
(13) Rogers, A. J.; Someya, T.; Huang, Y. Materials and Mechanics for Stretchable Electronics. *Science* **2010**, *327*, 1603−1607.

DOI: 10.1021/am508899z
ACS Appl. Mater. Interfaces 2015, 7, 7920−7926

(14) Park, M.; Park, J.; Jeong, U. Design of Conductive Composite Elastomers for Stretchable Electronics. *Nano Today* **2014**, *9*, 244−260.
(15) Sekitani, T.; Noguchi, Y.; Hata, K.; Fukushima, T.; Aida, T.; Someya, T. A Rubberlike Stretchable Active Matrix Using Elastic Conductors. *Science* **2008**, *321*, 1468−1472.
(16) Chun, K. Y.; Oh, Y.; Rho, J.; Ahn, J. H.; Kim, Y. J.; Choi, H. R.; Baik, S. Highly Conductive, Printable and Stretchable Composite Films of Carbon Nanotubes and Silver. *Nat. Nanotechnol.* **2010**, *5*, 853−857.
(17) Kim, Y.; Zhu, J.; Yeom, B.; Di Prima, M.; Su, X.; Kim, J.-G.; Yoo, S. J.; Uher, C.; Kotov, N. A. Stretchable Nanoparticle Conductors with Self-organized Conductive Pathways. *Nature* **2013**, *500*, 59−63.
(18) Park, M.; Im, J.; Shin, M.; Min, Y.; Park, J.; Cho, H.; Park, S.; Shim, M. B.; Jeon, S.; Chung, D. Y.; Bae, J.; Park, J.; Jeong, U.; Kim, K. Highly Stretchable Electric Circuits from a Composite Material of Silver Nanoparticles and Elastomeric Fibres. *Nat. Nanotechnol.* **2012**, *7*, 803−809.
(19) Khang, D.-Y.; Jiang, H.; Huang, Y.; Rogers, J. A. A Stretchable Form of Single Crystal Silicon for High Performance Electronics on Rubber Substrates. *Science* **2006**, *311*, 208−212.
(20) Gonzalez, M.; Axisa, F.; Bulcke, M. V.; Brosteaux, D.; Vandevelde, B.; Vanfleteren, F. Design of Metal Interconnects for Stretchable Electronic Circuits. *Microelectron Reliab.* **2008**, *48*, 825−832.
(21) Won, S. M.; Kim, H. S.; Lu, N.; Kim, D. G.; Del Solar, C.; Duenas, T.; Ameen, A.; Rogers, J. A. Piezoresistive Strain Sensors and Multiplexed Arrays Using Assemblies of Single-Crystalline Silicon Nanoribbons on Plastic Substrates. *IEEE Trans. Elec. Devices* **2011**, *58*, 4074−4078.
(22) Huang, X.; Liu, Y.; Cheng, H.; Shin, W. J.; Fan, J. A.; Liu, Z.; Lu, C. J.; Kong, G. W.; Chen, K.; Patnaik, D.; Lee, S. H.; Ali, S. H.; Huang, Y.; Rogers, J. A. Materials and Designs for Wireless Epidermal Sensors of Hydration and Strain. *Adv. Funct. Mater.* **2014**, *24*, 3846−3854.
(23) Ahn, B. Y.; Duoss, E. B.; Motala, M. J.; Guo, X.; Park, S.-I.; Xiong, Y.; Yoon, J.; Nuzzo, R. G.; Rogers, J. A.; Lewis, J. A. Omnidirectional Printing of Flexible, Stretchable, and Spanning Silver Microelectrodes. *Science* **2009**, *323*, 1590−1593.
(24) Siegel, A. C.; Bruzewicz, D. A.; Weibell, D. B.; Whitesides, G. M. Microsolidics: Fabrication of Three-Dimensional Metallic Microstructures in Poly(Dimethylsiloxane). *Adv. Mater.* **2007**, *19*, 727−733.
(25) Dickey, M. D.; Chiechi, R. C.; Larsen, R. J.; Weiss, E. A.; Weitz, D. A.; Whitesides, G. M. Eutectic Gallium-Indium (EGaIn): A Liquid Metal Alloy for the Formation of Stable Structures in Microchannels at Room Temperature. *Adv. Funct. Mater.* **2008**, *18*, 1097−1104.
(26) So, J. H.; Thelen, J.; Qusba, A.; Hayes, G. J.; Lazzi, G.; Dickey, M. D. Reversibly Deformable and Mechanically Tunable Fluidic Antennas. *Adv. Funct. Mater.* **2009**, *19*, 3632−3637.
(27) Kim, H.-J.; Maleki, T.; Wei, P.; Ziaie, B. A Biaxial Strechable Interconnect with Liquid-Alloy-Covered Joints on Elastomeric Substrate. *J. Microelectromech. Syst.* **2009**, *18*, 138−146.
(28) Park, Y. L.; Chen, B.; Wood, R. J. Soft Artificial Skin with Multi-Modal Sensing Capability Using Embedded Liquid Conductors. *Proc. IEEE Sensors* **2011**, *2*, 81−84.
(29) Majidi, C.; Kramer, R.; Wood, R. J. A Non-Differential Elastomer Curvature Sensor for Softer-than-Skin Electronics. *Smart Mater. Struct.* **2011**, *20*, 105017−105023.
(30) Cheng, S.; Wu, Z. Microfluidic Electronics. *Lab Chip* **2012**, *12*, 2782−2791.
(31) Park, J.; Wang, S.; Li, M.; Ahn, C.; Hyun, J. K.; Kim, D. S.; Kim, D. K.; Rogers, J. A.; Huang, Y.; Jeon, S. Three-Dimensional Nanonetworks for Giant Stretchability in Dielectrics and Conductors. *Nat. Commun.* **2012**, *3*, 916.
(32) Kramer, R. K.; Majidi, C.; Wood, R. J. Masked Deposition of Gallium-Indium Alloys for Liquid-Embedded Elastomer Conductors. *Adv. Funct. Mater.* **2013**, *23*, 5292−5296.
(33) Gozen, B. A.; Tabatabai, A.; Ozdoganlar, O. B.; Majidi, C. High-Density Soft-Matter Electronics with Micron-Scale Line Width. *Adv. Mater.* **2014**, *26*, 5211−5216.
(34) Liu, T.; Sen, P.; Kim, C.-J. Characterization of Nontoxic Liquid-Metal alloy Galinstan for Applications in Microdevices. *J. Microelectromech. Syst.* **2012**, *21*, 443−450.
(35) Regan, M.; Tostmann, H.; Pershan, P. S.; Magnussen, O.; DiMasi, E.; Ocko, B.; Deutsch, M. X-ray Study of the Oxidation of Liquid-Gallium Surfaces. *Phys. Rev. B* **1997**, *55*, 10786−10790.
(36) Dumke, M. F.; Tombrello, T. A.; Weller, R. A.; Housley, R. M.; Cirlin, E. H. Sputtering of the Gallium-Indium Eutectic Alloy in the Liquid Phase. *Surf. Sci.* **1983**, *124*, 407−422.
(37) Scharmann, F.; Cherkashinin, G.; Breternitz, V.; Knedlik, C.; Hartung, G.; Weber, T.; Schaefer, J. A. Viscosity Effect on GaInSn Studied by XPS. *Surf. Interface Anal.* **2004**, *36*, 981−985.
(38) Scharmann, F.; Cherkashinin, G.; Breternitz, V.; Knedlik, C.; Hartung, G.; Weber, T.; Schaefer, J. A. Viscosity Effect on GaInSn Studied by XPS. *Surf. Interface Anal.* **2004**, *36*, 981−985.
(39) Kim, D.; Lee, D.-W.; Choi, W.; Lee, J.-B. A Super-Lyophobic 3-D PDMS Channel as a Novel Microfluidic Platform to Manipulate Oxidized Galinstan. *J. Microelectromech. S.* **2013**, *22*, 1267−1275.
(40) Zheng, Y.; He, Z.; Gao, X.; Liu, J. Direct Desktop Printed-Circuits-on-Paper Flexible Electronics. *Nat. Commun.* **2013**, *3*, 1786.
(41) Fassler, A.; Majidi, C. 3D Structures of Liquid-Phase GaIn Alloy Embedded in PDMS with Freeze Casting. *Lab Chip* **2013**, *13*, 4442−4450.
(42) Ladd, C.; So, J. H.; Muth, J.; Dickey, M. D. 3D Printing of Free Standing Liquid Metal Microstructures. *Adv. Mater.* **2013**, *25*, 5081−5085.
(43) Kim, T. Y.; Kim, Y. W.; Lee, H. S.; Kim, H.; Yang, W. S.; Suh, S. Uniformly Interconnected Silver-Nanowire Networks for Transparent Film Heaters. *Adv. Funct. Mater.* **2013**, *23*, 1250−1255.
(44) Moon, G. D.; Lim, G.; Song, J. H.; Shin, M.; Yu, T.; Lim, B.; Jeong, U. Highly Stretchable Patterned Gold Electrodes Made of Au Nanosheets. *Adv. Mater.* **2013**, *25*, 2707.
(45) Sivan, V.; Tang, S. Y.; O'Mullane, A. P.; Petersen, P.; Eshtiaghi, N.; Kalantar-zadeh, K.; Mitchell, A. Liquid Metal Marbles. *Adv. Funct. Mater.* **2013**, *23*, 144−152.
(46) Kim, D.; Lee, Y.; Lee, D.-W.; Choi, W.; Lee, J.-B. J. Hydrochloric Acid-Impregnated Paper for Liquid Metal Microfluidics. *Transducers Eurosens. XXVII, Int. Conf. Solid-State Sens., Actuators Microsyst., 17th* **2013**, 2620−2623.
(47) de Gennes, P.-G.; Brochard-Wyart, F.; Quéré, D. *Capillarity and Wetting Phenomena: Drops, Bubbles, Pearls, Waves*; Springer: Berlin, 2003; pp 69−70.
(48) Xiu, Y.; Zhu, L.; Hess, D. W.; Wong, C. P. Relationship between Work of Adhesion and Contact Angle Hysteresis on Super-hydrophobic Surfaces. *J. Phys. Chem. C* **2008**, *112*, 11403−11407.
(49) Chaudhury, M. K.; Whitesides, G. M. Direct Measurement of Interfacial Interactions between Semispherical Lenses and Flat Sheets of Poly(Dimethylsiloxane) and Their Chemical Derivatives. *Langmuir* **1991**, *7*, 1013−1025.
(50) Wang, J. Z.; Zheng, Z. H.; Li, H. W.; Huck, W. T. S.; Sirringhaus, H. Dewetting of Conducting Polymer Inkjet Droplets on Patterned Surfaces. *Nat. Mater.* **2004**, *3*, 171−176.
(51) Oh, J. Y.; Shin, M.; Lee, J. B.; Ahn, J.-H.; Baik, H. K.; Jeong, U. Effect of PEDOT Nanofibril Networks on the Conductivity, Flexibility, and Coatability of PEDOT:PSS Films. *ACS Appl. Mater. Interfaces* **2014**, *6*, 6954−6961.
(52) Reeves, G. K.; Harrison, H. B. Obtaining the Specific Contact Resistance from Transmission Line Model Measurements. *Electron Devic. Lett.* **1982**, *3*, 111−113.
(53) Park, Y.-L.; Chen, B.-R.; Wood, R. J. Design and Fabrication of Soft Artificial Skin Using Embedded Microchannels and Liquid Conductors. *IEEE Sens. J.* **2012**, *12*, 2711−2718.
(54) Moon, G. D.; Lee, T.-I.; Kim, B.; Myoung, J.; Jeong, U. Assembled Monolayers of Hydrophilic Particles on Water Surfaces. *ACS Nano* **2011**, *5*, 8600−8612.

DOI: 10.1021/am508899z
ACS Appl. Mater. Interfaces 2015, 7, 7920−7926